ADVANCED FUNCTIONAL MATERIALS

Supporting Information

for *Adv. Funct. Mater.,* DOI: 10.1002/adfm.201600210

An Underwater Surface-Drying Peptide Inspired by a Mussel Adhesive Protein

Wei Wei, *Luigi Petrone*, *YerPeng Tan*, *Hao Cai*, *Jacob N. Israelachvili*, *Ali Miserez*, *and J. Herbert Waite**

Supporting Information

An Underwater Surface Drying Peptide Inspired by a Mussel Adhesive Protein

Wei Wei[1]‡, Luigi Petrone[2]‡, YerPeng Tan[4], Hao Cai[2], Jacob N. Israelachvili[1,4], Ali Miserez[2,3], J. Herbert Waite[1,4]*

[1] Materials Research Lab, University of California, Santa Barbara

[2] School of Materials Science and Engineering, Nanyang Technological University, Singapore

[3] School of Biological Sciences, Nanyang Technological University, Singapore

[4] Biomolecular Science and Engineering Program, University of California, Santa Barbara

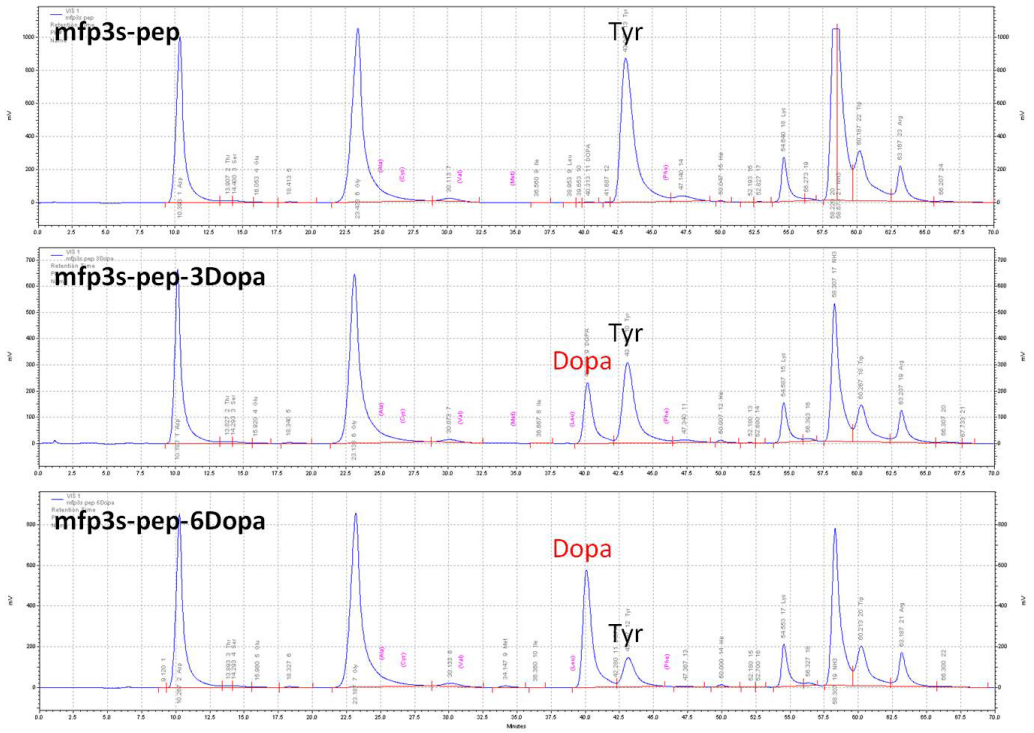

Figure S1. Amino acid analyses of mfp3S-pep, mfp3S-pep-3Dopa and mfp3S-pep-6Dopa.

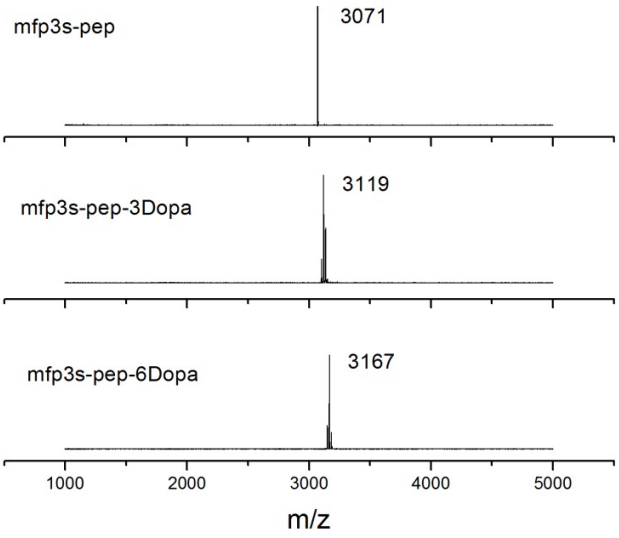

Figure S2. MALDI-TOF-MS spectra of mfp3S-pep, mfp3S-pep-3Dopa, and mfp3S-pep-6Dopa after enzymatic hydroxylation by tyrosinase.

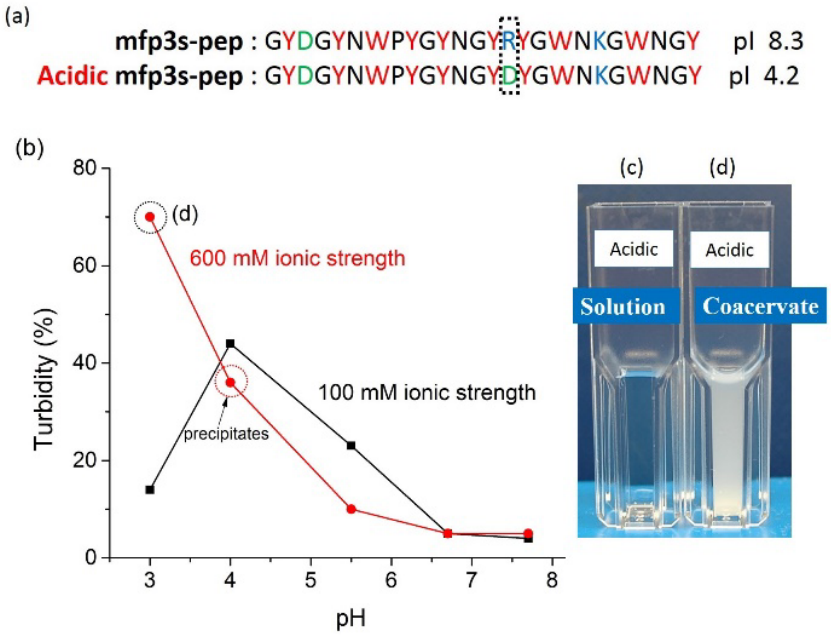

Figure S3. (a) Acidic (R→D) version of mfp3S-pep sequence; (b) acidic-mfp3S-pep turbidity under different pH and ionic strength conditions; (c, d) comparison of acidic-mfp3S-pep solution and coacervate.

mfp3s-pep: GYDGYNWPYGYNGY RYGWNKGWNGY

Mfp3s-pep-random #1: NGPGGGYYYGWYKRYYYGWNNWNGD
maximum solubility in 10 mM acetic acid: **0.2 mg/ml**

Mfp3s-pep-random #2: GNGYGYNNYRYWGNKWYPYGGDGYW

Mfp3s-pep-random #3: PGNWNRNGYYNWGDYGWYGKGYGYY
maximum solubility in 10 mM acetic acid < **1 mg/ml**

Figure S4. Mfp3S-pep with 3 randomized sequences and relative solubility in 10 mM acetic acid. Mfp3S-pep-random #2 is boxed to indicate that it was the only randomized sequence able to self-coacervate as mfp3S-pep. (The original sequence mfp3S-pep and mfp3S-pep-random #2 both have solubility higher than 2 mg/ml.)

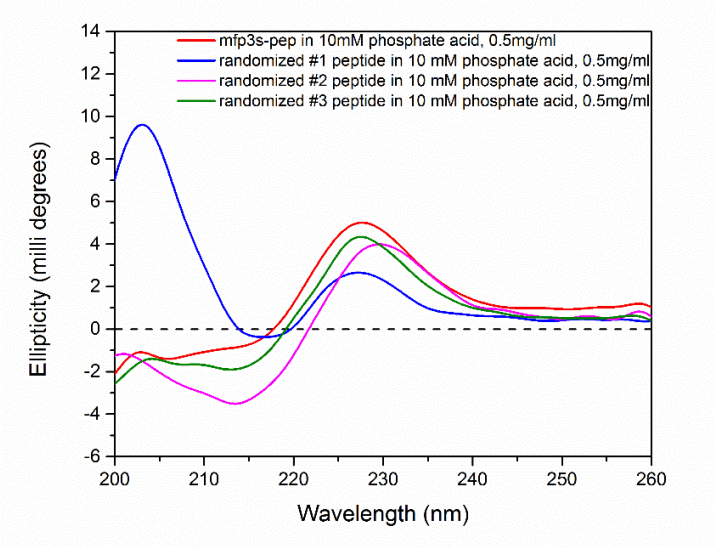

Figure S5. CD spectra of Mfp3s-pep and Mfp3s-pep-random #1, 2, 3 in 10 mM phosphoric acid solution.

	Mfp3s-pep
Sequence	GYDGYNWPYGYNGYRYGWNKGWNGY
Prediction	CCCCCCCCCCCCCSSSCCCCCCCCC
Conf.Score	97664377534653402335666 79
	H:Helix; S:Strand; C:Coil

	random #2
Sequence	GNGYGYNNYRYWGNKWYPYGGDGYW
Prediction	CCCCCCCCSSSCCCCCCCCCCCCC
Conf.Score	98545144041044000368776 69
	H:Helix; S:Strand; C:Coil

	random #1
Sequence	NGPGGGYYYGWYKRYYYGWNNWNGD
Prediction	CCCCCCSSSSSSSSSSSCCCCCCCC
Conf.Score	98876236666787783123557 89
	H:Helix; S:Strand; C:Coil

	random #3
Sequence	PGNWNRNGYYNWGDYGWYGKGYGYY
Prediction	CCCCCCCCCCCCCCCCCCCCCCCCC
Conf.Score	98545465111444341414423 59
	H:Helix; S:Strand; C:Coil

Figure S6. Predicted secondary structures of mfp3s-pep and mfp3s-pep-random #1, 2, 3 using I-Tasser model.

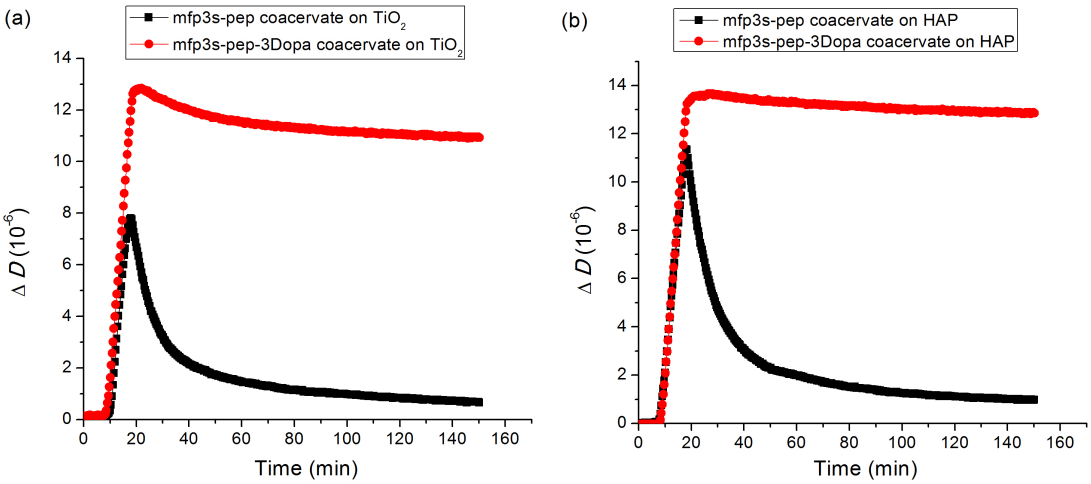

Figure S7. Mfp3S-pep, mfp3S-pep-3Dopa coacervates adsorption behavior on HAP and TiO_2 surface in QCM-D experiments: dissipation change after exposing (a) TiO_2 and (b) HAP to peptides.

ATR-IR spectroscopic study of dopamine in solution and adsorbed on TiO_2 and HAP.

Dopamine was selected as a model compound bearing a catechol group for ATR-IR adsorption studies on TiO_2 and HAP nanoparticle films. The information about the characteristic absorptions of the catechol moiety both in solution and as an adsorbate on the two investigated surfaces assisted in the band assignments of the more complex Dopa-containing peptide and coacervate in this work.

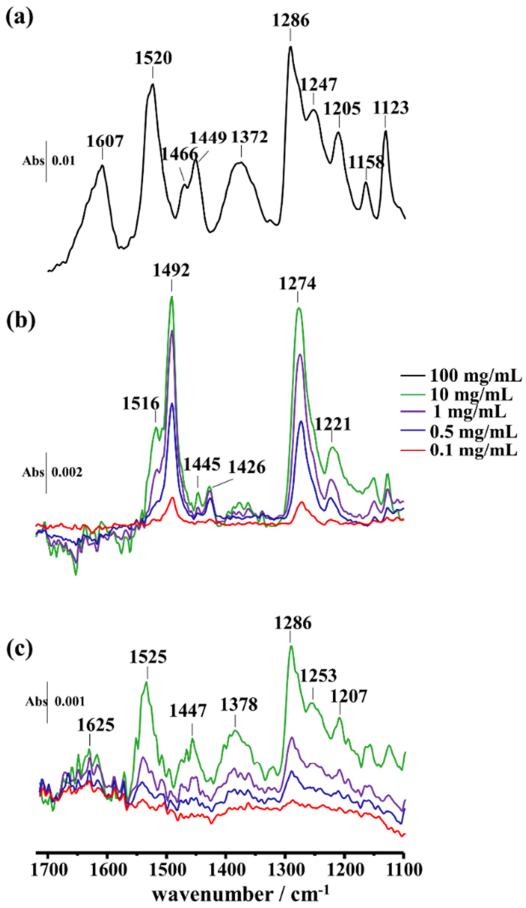

Figure S8. ATR-IR spectra of dopamine in 100 mM acetic acid aqueous solution on (a) bare ZnSe prism at 100 mg/mL (black trace); (b) adsorbed on TiO_2 and (c) HAP at 10 (green trace), 1 (indigo trace), 0.5 (blue trace) and 0.1 mg/mL (red trace). Background in a, b, c are from 100 mM acetic acid on ZnSe prism, on TiO_2- and on HAP-coated ZnSe prism, respectively.

The ATR-IR spectrum of 100 mg/mL dopamine in 100 mM acetic acid solution on the bare ZnSe prism is presented in Figure S7a. More dilute dopamine solutions were also tested but the absorbances were weak and not discernible, whereas spectra of adsorbed dopamine at 100 mg/mL resulted in well-resolved and intense absorptions. The band peaking at 1607 cm^{-1} originated from the bending mode (δ) of OH groups of water molecules hydrating the adsorbed dopamine. The absorption at 1520 cm^{-1} was attributed to a combination mode of ν(CC)+δ(CH) of free catechol species in solution ($catechol_{aq}$)[37,53]. Bands observed between 1400 and 1480 cm^{-1} were from vibrations of the CH_2 groups[54], and peaks at 1372 and 1205 cm^{-1} were assigned to δ(OH) vibrational modes of catechol groups[53,55]. Other catechol absorptions at 1286 and 1247

cm^{-1} originated from the ν(CO) mode, whereas bands at 1158 and 1123 cm^{-1} were assigned to δ(CH) and δ(CH)+δ(OH) modes[37,53,56,57], respectively. The ν(NH) mode of the primary amine in dopamine was observed at higher wavenumbers peaking at ~3300 cm^{-1} (not shown).Subsequently, the ZnSe prism was coated with either TiO_2 or HAP nanoparticle films in order to investigate the adsorption mechanism of dopamine on these surfaces. A 100 mM aqueous acetic acid solution was initially flowed over the particle-coated prism, and a background was recorded. Thereafter, dopamine solutions of 0.1, 0.5, 1 and 10 mg/mL were passed over the investigated nanoparticle films and the ATR-IR spectra were recorded (Figures S7b and S7c). The spectral absorbances increased with the dopamine concentrations and were already detectable on TiO_2 at the lowest concentration of 0.1 mg/mL. Weaker yet discernible absorbances were recorded on HAP at 0.5 mg/mL dopamine concentration. The characteristic doublet indicative of catechol-Ti(IV) bidentate binuclear coordinative bond was found at 1492 and 1274 cm^{-1} [37,38]. The ATR-IR spectrum of dopamine adsorbed on HAP showed similarities in terms of bands number and position to the $catechol_{aq}$ spectrum recorded at a concentration 100 mg/mL without any nano particulate layer. The major absorbance peaking at 1286 cm^{-1} and its shoulder at ~1250 cm^{-1} (1247 cm^{-1} in Figure S3a and 1253 cm^{-1} in Figure S3c) were thus assigned to the ν(CO) mode associated with $catechol_{aq}$. The absorption in Figure S3c peaking at 1525 cm^{-1} was associated with the ν(CC)+δ(CH) mode, as previously observed for the $catechol_{aq}$ spectrum (absorption at 1520 cm^{-1}). This absorption was discernible in the ATR-IR spectra of dopamine adsorbed on TiO_2 as a shoulder of the peak at 1492 cm^{-1} from a concentration of 0.5 mg/mL, which then became more prominent at higher concentrations as a distinct peak at 1516 cm^{-1}. To summarise, dopamine formed a coordinative bond via the *o*-hydroxyl groups with the Ti(IV) atoms of the TiO_2 anatase surface, which was apparent as a doublet at 1492 and 1274 cm^{-1}.

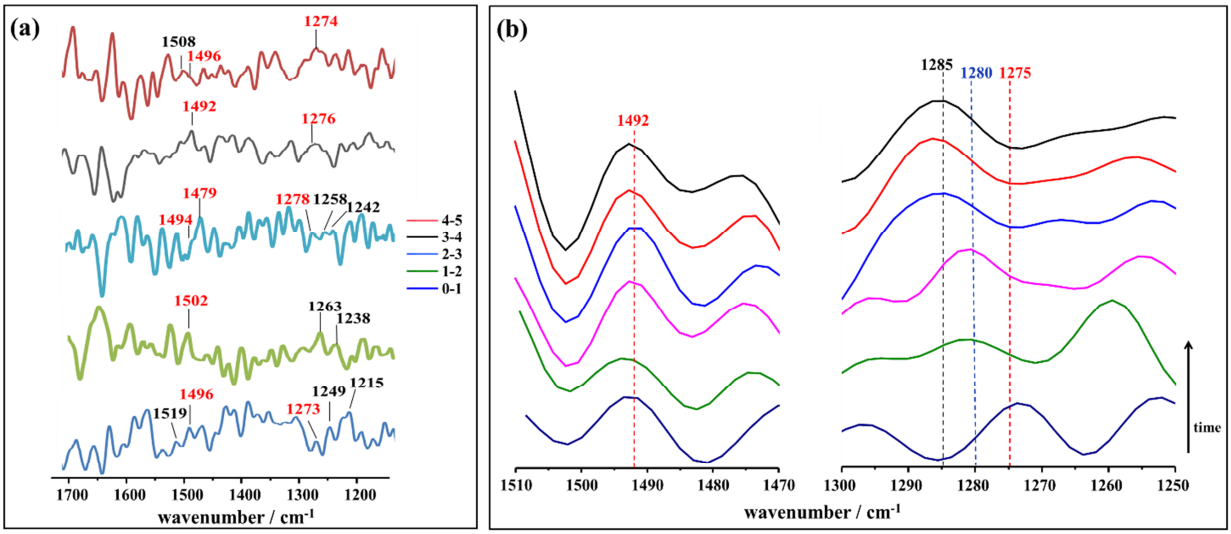

Figure S9. (a) ATR-IR difference spectra for mfps-pep-3Dopa coacervate adsorbed on TiO_2 obtained by subtracting consecutive normalized ATR-IR spectra in Figure 5c. (b) Evolution of the negative second-derivative spectra of mfps-pep-3Dopa adsorbed on TiO_2 in the 1505-1475 cm^{-1} and 1300-1255 cm^{-1} spectral regions. Peaks characteristic of catechol-Ti(IV) coordinative bond, an intermediate surface structure, and outer-sphere complex are indicated by the red, blue and black dotted lines, respectively.

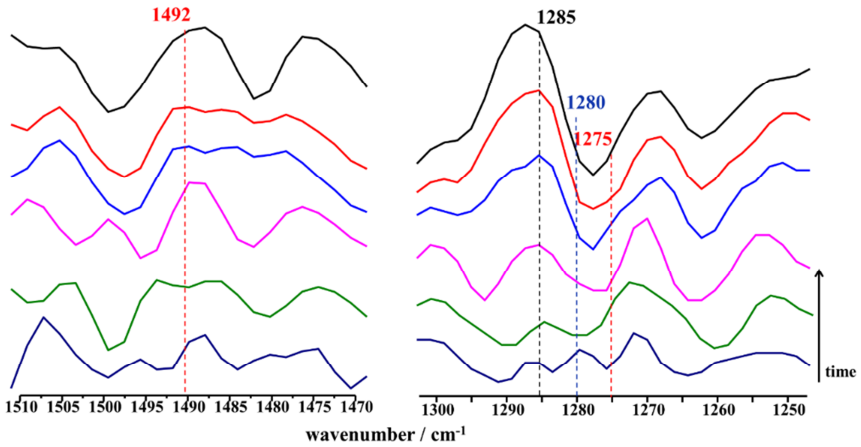

Figure S10. Evolution of the negative second-derivative spectra of mfps-pep-3Dopa adsorbed on HAP in the 1505-1475 cm^{-1} and 1300-1255 cm^{-1} spectral regions. Peaks characteristic of catechol coordinative bond, an intermediate surface structure, and outer-sphere complex are indicated by the red, blue and black dotted lines, respectively.

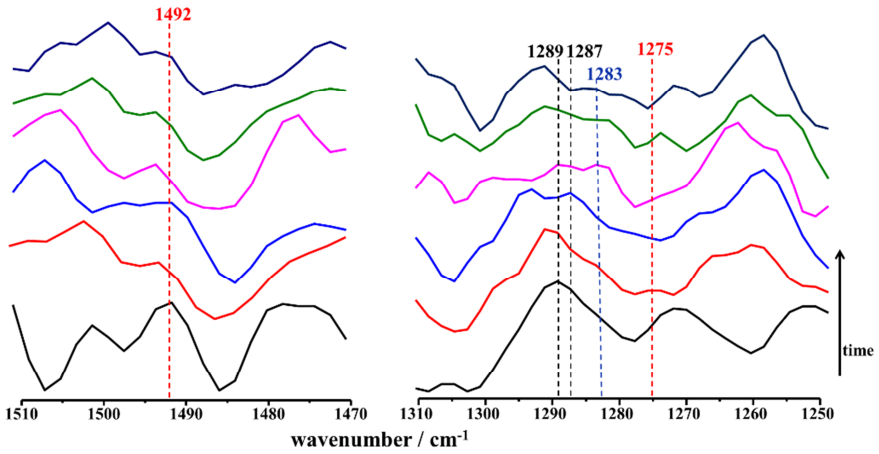

Figure S11. Evolution of the negative second-derivative spectra of mfps-pep-3Dopa coacervate adsorbed on HAP in the 1505-1475 cm^{-1} and 1300-1255 cm^{-1} spectral regions. Peaks characteristic of catechol coordinative bond, an intermediate surface structure, and outer-sphere complex are indicated by the red, blue and black dotted lines, respectively.

Peptides' Conformational transition during adsorption by ATR-FTIR

The amide I band in the ATR-IR spectra of adsorbed mfp3S-pep on TiO_2 (Fig. 7a) showed a peak at 1660 cm^{-1} in all recorded spectra. This peak is indicative of the concomitant presence of α-helix and β-turn structures peaking at about 1656 and 1667 cm^{-1}, respectively. Structural changes are inevitable whenever peptides interact either specifically or nonspecifically with a substrate due to the formation of new bonds and variation in the centre of symmetry of functional groups, giving rise to new peaks or shifts of bands. However, the position of the band maximum and its shape did not change upon adsorption of the peptide from solution over time, which is consistent with the peptide's inability to displace surface-adsorbed water, and thus to interact with the underlying surface.

The amide I band from adsorbed mfp3S-pep-3Dopa on TiO_2 (Fig. 7b) exhibited a maximum at about 1647 cm^{-1} along with a broader shoulder at lower wavelengths consistent with both random and β-sheet secondary structures, respectively. The contribution from β-sheets to the

amide I band became more evident over the course of the adsorption (a peak gradually becoming more intense with time at lower wavelengths of the amide I band), pointing to a conversion of random structures into β-sheets as the peptide interacted with the titania surface.

Lastly, the coacervated peptide showed well-resolved peaks within the amide I from its adsorption on the same surface (Fig. 5c). The two peaks in the first spectrum can be attributed to the concomitant presence of α-helix and β-turn (about 1660 cm^{-1}) and β-sheet (about 1625 cm^{-1}) structures. Over time, the two peaks merged into one band at 1656 cm^{-1}, which is indicative of α-helices only.

On the HAP surface, all three ATR-IR adsorption studies (Fig. 10) gave comparable results to those obtained on TiO_2. In summary, the shape and evolution of the amide I band in the adsorption experiments confirmed that the peptide without Dopa was not able to effectively interact with the TiO_2 surface, whilst mfp3S-pep-3Dopa revealed structural rearrangements during the adsorption process both in solution and as a coacervate.